ELSEVIER

Finite Elements in Analysis and Design 30 (1998) 19–30

FINITE ELEMENTS IN ANALYSIS AND DESIGN

Thermal-mechanical interface crack behaviour of a surface mount solder joint

C.M.L. Wu[a,*], J.K.L. Lai[a], Yong-li Wu[b]

[a] Department of Physics and Materials Science, City University of Hong Kong, Hong Kong, People's Republic of China

[b] Institute of Mechanics, Chinese Academy of Sciences, Beijing 100080, People's Republic of China

Abstract

The effect of thermal-mechanical loading on a surface mount assembly with interface cracks between the solder and the resistor and between the solder and the printed circuit board (PCB) was studied using a non-linear thermal finite element analysis. The thermal effect was taken as cooling from the solder eutectic temperature to room temperature. Mechanical loading at the ends of the PCB was also applied. The results showed that cooling had the effect of causing large residual shear displacement at the region near the interface cracks. The mechanical loading caused additional crack opening displacements. The analysis on the values of J-integral for the interface cracks showed that J-integral was approximately path independent, and that the effect of crack at the solder/PCB interface is much more serious than that between the component and solder. © 1998 Elsevier Science B.V. All rights reserved.

Keywords: Lead–tin solder joint; Thermal-mechanical analysis; J-integral; Finite element analysis; Interface crack

1. Introduction

Surface mount technology (SMT) has been developed to enable the production process to be automated, to reduce product size and to lower the production cost. It is currently implemented as a leading electronic packaging and interconnect assembly process. One of the widely used surface mount component is the Leadless Ceramic Chip Carriers (LCCC). However, some LCCC solder joints have suffered from poor reliability, which depends on many parameters such as the soldering temperature, the wetability, the composition of the solder, the geometry of the solder joint and many other environmental factors.

A surface mount assembly is basically a composite structure consisting of three major parts: the printed circuit board (PCB), the solder joints, and the electronic component. In a surface mount

* Corresponding author.

0168-874X/98/$19.00 © 1998 Elsevier Science B.V. All rights reserved

PII S0168-874X(98)00028-6

package, materials with different thermal and mechanical properties are bonded together to constitute a complicated system. The material properties may change unintentionally due to the bonding process and/or service environment. Also, the interfaces between different materials, e.g. in the present case the ceramic/solder and the solder/PCB interfaces, inevitably contain stress gradients and even stress singularities, especially at the locations near the free surfaces. Such stress concentration areas are attributed to thermal expansion as well as stiffness mismatch of the bonded materials and can always provide a source of crack initiation [1]. Moreover, voids and microcracks can be found along or very close to the interface and may further develop into large cracks that lead to the failure of the package. Understanding the behaviour of cracks along bi-material interfaces thus plays an important role in achieving higher reliability in a surface mount package.

Numerous power cycling experiments have been performed in order to investigate solder joint reliability [2–8]. Clatterbaugh and Charles [8] also studied the effect of the solder joint geometry by finite element analysis. They suggested that the solder joint geometry may have a major influence on joint reliability under thermal cycling conditions. Lau et al. [9] analyzed a surface-mount assembly with a 1206 ceramic chip resistor, an FR-4 epoxy/glass PCB and a 63 wt%Sn–37 wt%Pb solder joint using the finite element method. They found that the standoff height of the solder joint affected the strain distribution and the maximum shear strain for all cases occurred near the knee of the solder joint, i.e. the corner interface of the chip resistor and the solder joint (see Fig. 1). Their finite element analysis also included the elasto-plastic properties of the solder. A temperature difference of 180°C (from -55°C to 125°C) was considered in their analysis.

Yamada [10,11] investigated analytically and experimentally the fracture behaviour in a thin elasto-plastic layer bonded by elastic beam-like materials. The direct impetus of his study was to investigate the cracking of a solder joint commonly seen in electronic systems [12]. Kokini and Reynolds [13] investigated the effect of transient heating and cooling on an interface crack between a ceramic and a metal which were reasonably homogeneous, isotropic and linear-elastic.

In this paper, the effect of cooling and the application of external forces on interface cracks at the ceramic/solder and solder/PCB interfaces of a surface mount assembly was investigated. Unlike the ceramic-to-metal bond investigated by Kokini and Reynolds [13], the solder yielded at a low stress level. Naturally, the linear elastic fracture mechanics (LEFM) approach [14] developed for interface crack is not directly applicable for solder joints. The J-integral introduced by Rice [15] is the most widely recognised fracture parameter for elasto-plastic fracture problems of homogeneous materials. Smelser and Gurtin [16] have shown that J-integral is path independent for bi-material bodies when the interface is linear.

Yamada [17] used the J-integral in the study of solder joint cracking. In the present analysis, a finite element code, ABAQUS, was employed to study the thermal transient fracture analysis. The

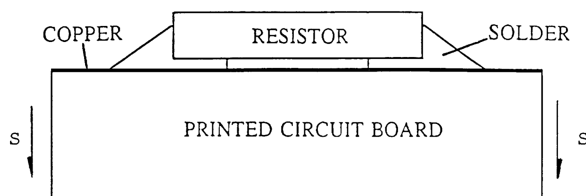

Fig. 1. A surface-mounted assembly.

thermal-mechanical deformations and the variation of the J-integral for the interface crack of the surface mount solder joints were obtained.

2. Description of the problem

The configuration of a surface mount assembly is shown in Fig. 1. The assembly consists of a ceramic resistor, the solder and an FR-4 epoxy/glass PCB that has a copper layer on the top surface for electrical conduction. For the present analysis, the ceramic, FR-4 and copper are assumed to be linear-elastic. The solder is assumed to be isotropic and under isotropic hardening rule. The Ramberg–Osgood equation has been used to describe the elasto-plastic stress–strain behaviour of the solder, viz.

$$\varepsilon = \frac{\sigma}{E} + \beta\left(\frac{\sigma}{\sigma_y}\right)^n, \tag{1}$$

where $\beta = 0.001$ and $n = 10$. The physical and mechanical properties of the material, density ρ, specific heat c, thermal conductivity κ, thermal expansion coefficient α, modulus of elasticity E, Poisson's ratio v and yield strength σ_y are shown in Table 1 [18,19].

It is assumed that during soldering the whole assembly is stress free until just under the solder eutectic temperature of 183°C. It is also assumed that there is an initial crack after soldering. Since studies by past investigators [1,2] identified initiation of cracks were likely to be at the solder/resistor and solder/PCB interfaces, two cases of interface cracks were considered for this study. In Case 1, an interface crack between the resistor and the solder is modelled. Case 2 is with an interface crack between the solder and the PCB. Initially the cracked joints in both cases are subjected to cooling from the eutectic temperature of 183°C to room temperature of 22°C. Then external forces in the form of shear forces at the ends of the PCB are applied. The effects due to the thermal-mechanical loading on the interface cracks is studied.

As mentioned before, the solution was obtained using the ABAQUS finite element code [20]. Because of the symmetry of the geometry and the initial temperature field, it was only necessary to analyse half of the structure. The finite element model contained 467 elements which were 8-noded isoparametric quadrilaterals. The general mesh configurations for Case 1 and Case 2 are shown in

Table 1
Material properties for the assembly

	Ceramic	Sn63/Pb37	Copper	FR-4
ρ (10^{-3} g/mm^3)	3.72	8.41	8.94	3.0
c J/(g K)	0.774	0.1498	0.3815	0.1
κ (W/(mm K))	0.0251	0.04979	0.3978	0.0002622
α (10^{-6}/K)	6.2	24.0	16.12	9.9
E (MPa)	303400.0	30752.0	132400.0	16275.0
v	0.21	0.4	0.34	0.12
σ_y (MPa)	344.75	31.03	68.95	50.0

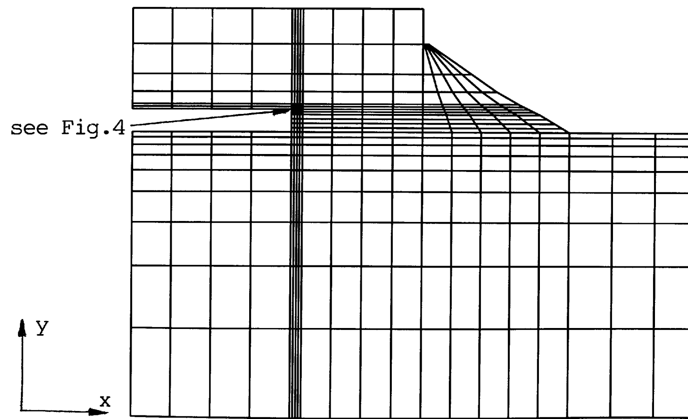

Fig. 2. Finite element mesh for Case 1.

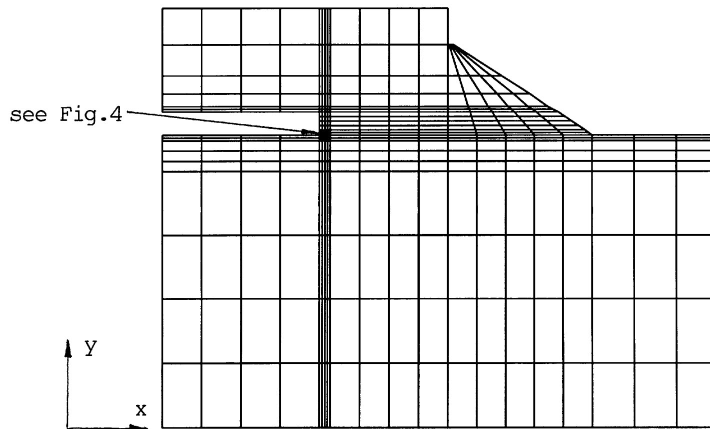

Fig. 3. Finite element mesh for Case 2.

Figs. 2 and 3. The mesh is progressively refined near the crack tips as shown in Fig. 4. A total of 1450 nodes were used in the model. In the first instance, the transient temperature distribution was obtained. Subsequently, the displacement at successive time increments were computed. The crack faces were prevented from interpenetrating by using interface elements which were assumed to provide frictionless contact [20].

3. Theory

Rice [15] formulated the solution for the stress and strain fields existing in a crack tip plastic zone in terms of J and a hardening exponent, n. The definition of J relates to a non-linear elastic material, which behaves identically during loading to a material which follows a total or deformation plasticity constitutive law. For monotonic loading only, deformation and incremental plasticity theories provide very similar results [21]. In the present analysis the solder is assumed to cool

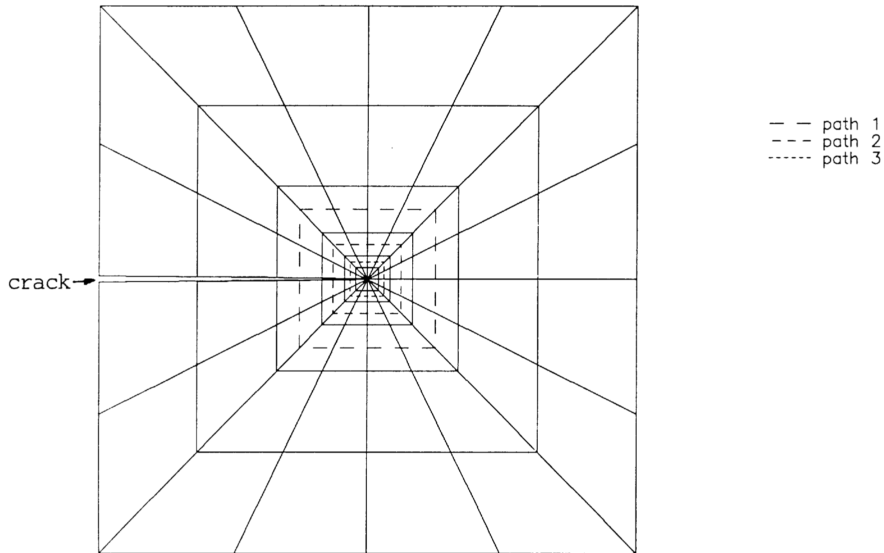

Fig. 4. Finite element mesh at the region with interface crack.

down from the eutectic temperature to room temperature. It is therefore reasonable to assume that the resulting internal stresses in the solder material will be monotonic and the use of the J-integral is justified. The J-integral is expressed by [15]

$$J = \int_{\Gamma} W \, \mathrm{d}y - n_i \sigma_{ij} \frac{\partial u_j}{\partial x} \, \mathrm{d}s \tag{2}$$

in which Γ is any contour from the bottom crack surface around the crack tip to the top surface, σ_{ij} is the stress tensor, u_i the displacement vector, n_i the outward unit normal to the contour, and W the strain energy density expressed by

$$W = \int_0^{\varepsilon_{ij}} \sigma_{ij} \, \mathrm{d}\varepsilon_{ij}. \tag{3}$$

The value of J is independent of the actual path, Γ, chosen provided that the initial and end points of the contour are on opposite faces of the crack and that the crack faces are stress free. The concept of a path independent J-integral holds vigorously only for non-linear elastic materials, in which case

$$J = -\frac{\partial P}{\partial a}, \tag{4}$$

where P is the potential energy per unit thickness and a is the crack length. For linear-elastic expressions $J = G$, the strain energy release rate with crack advances.

J plays the same role in elasto-plastic fracture as does K, the stress intensity factor, in LEFM and crack advance can be monitored in terms of a critical value J_c. The stress and strain ahead of a crack can be determined principally by the value of J. If a critical crack tip stress field is required

to initiate fracture, the value of $J = J_c$ specifies this stress. Similarly, if the fracture mechanism is strain controlled then J characterises the critical strain conditions ahead of the crack at failure.

4. Results and discussion

It was identified in microstructural examinations that defect size in surface mount solder joints ranged from 0.001 to 0.05 mm. So results were calculated for a crack length, a, of 0.03 mm which was within the range between 0.001 and 0.05 mm. The heat transfer coefficients h_c of microelectronic packages for convection cooling depend upon many factors, such as surface geometry and texture, fluid velocity and temperature and surface inclination. Dean [19] gave the range of values measured, $h_c = 0.0005$–0.0025 W/(cm^2 K). In this paper, the typical value of $h_c = 0.001$ W/(cm^2 K) was used.

In each case, after cooling from the eutectic temperature to room temperature, shear forces, S, as shown in Fig. 1 were applied. Various values of S were taken and these are shown in Table 2. It is noted that the vertical displacements at the axis of symmetry of the assembly were fixed.

Table 2
Magnitudes of force S

	S/S_0 ($S_0 = 50$ MPa)
Step 0	0
Step 1	0.1
Step 2	0.2
Step 3	0.35
Step 4	0.575
Step 5	0.913
Step 6	1.0

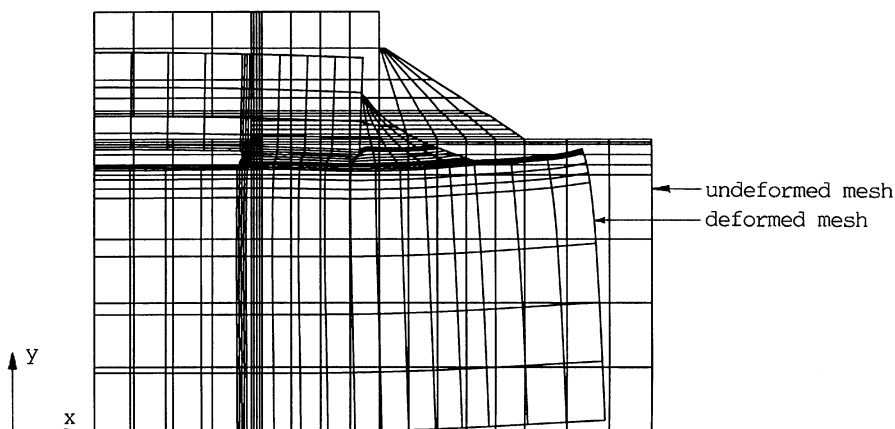

Fig. 5. Undeformed and deformed mesh for Case 1, load step 0.

In Case 1, the crack was modelled between the resistor and the solder, as shown in Fig. 2. Fig. 5 shows the global deformation of the surface mount component due to the temperature change from the eutectic temperature to room temperature without the external force, i.e., Step 0. It can be seen that as a result of the temperature change, the PCB bent upward at the ends and produced crack opening at the resistor/solder interface. Fig. 6 shows the local deformation of the interface crack. The details of the displacement y around the crack region for Step 0 can be found in Fig. 7. It can be seen that the crack was opened for about 0.00012 mm at the edge of the resistor/solder interface. From Figs. 6 and 7 it can also be seen from the displacements at the open end of the crack that it was opened and sheared. In particular, the bottom surface was sheared more to the right.

When progressively increasing magnitude of shear force S is applied, the deformation of the PCB in relation to the component becomes larger. This behaviour can be seen in Fig. 8 for Step 6 for

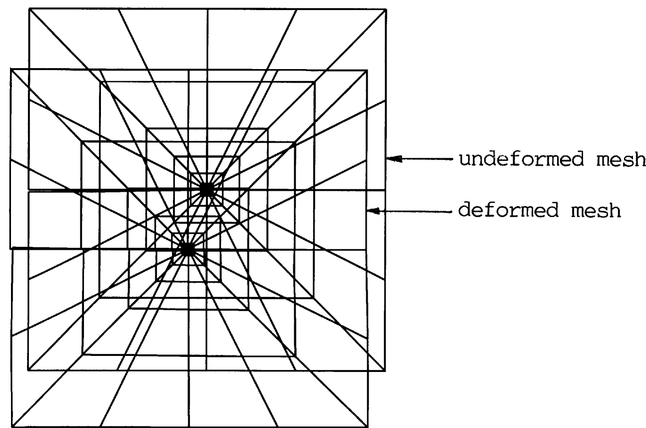

Fig. 6. Undeformed and deformed mesh at the region with the interface crack for Case 1, load step 0.

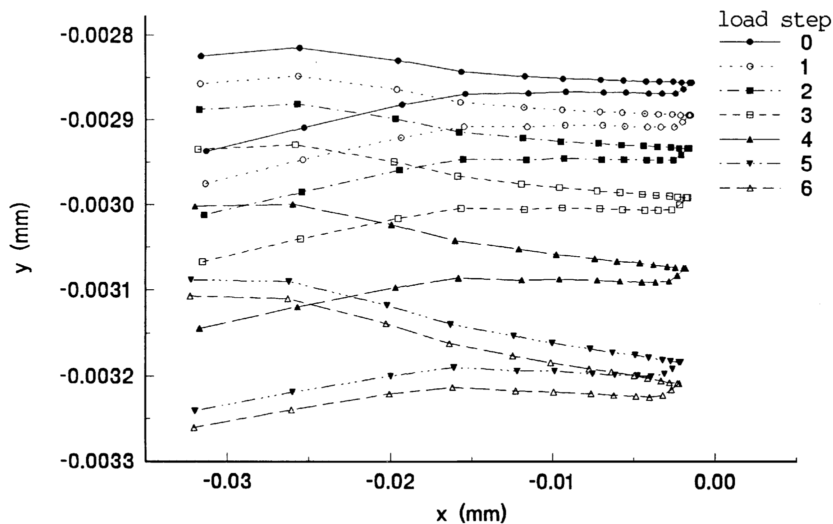

Fig. 7. Deformation of interface crack for Case 1.

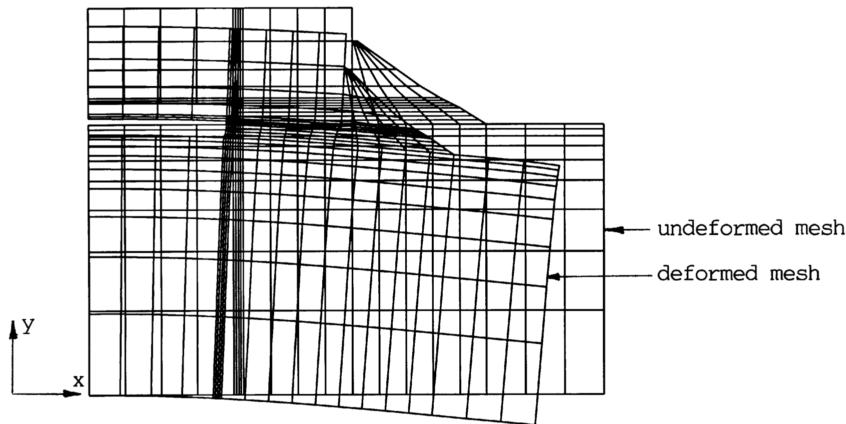

Fig. 8. Undeformed and deformed meash for Case 1, load step 6.

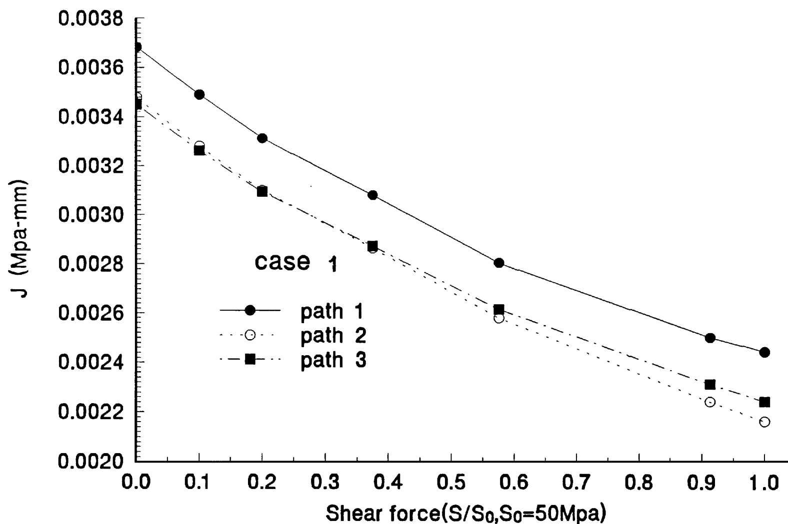

Fig. 9. Variation of J-Integral with shear force for Case 1.

Case 1. The large deformation is clearly visible by comparing this figure with Fig. 5. The deformation of the cracked surfaces for all load steps are compared in Fig. 7. The deformation is seen to increase with the increase in S.

Using the magnitude of S in load steps 0 to 6, the variation between the J-integral with shear force is shown in Fig. 9. The J-integral decreases with the increase in shear force. The evaluation of the value of J-integral was obtained along three integration paths, as shown in Fig. 4, and their values are shown in the same figure. It can be seen that the maximum difference is only about 5%, although the difference becomes slightly larger as the shear force is increased. The J-integral is considered to be approximately path independent.

For Case 2, the crack was modelled between the solder and the PCB, as shown in Fig. 3. The deformation of the assembly for load Step 0 is shown in Fig. 10. Again the PCB was bent upward at

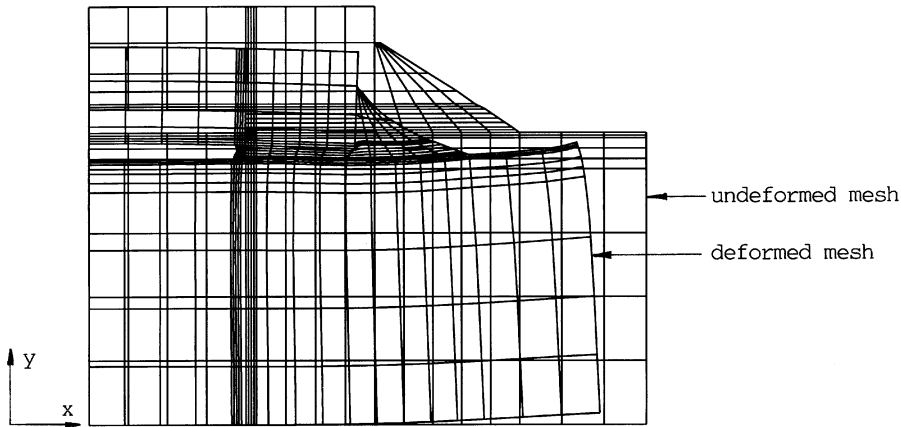

Fig. 10. Undeformed and deformed mesh for Case 2, load step 0.

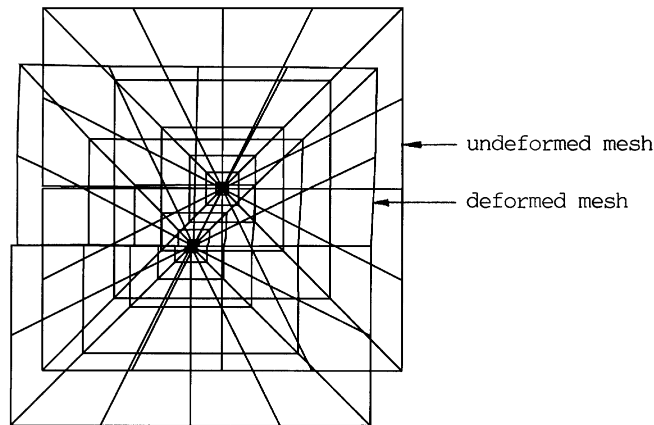

Fig. 11. Undeformed and deformed mesh a the interface crack for Case 2, load step 0.

the end, creating a bending moment and providing crack opening. Fig. 11 shows the deformation near the crack tip. The deformation pattern at the crack tip at various load steps are compared in Fig. 12. It can be seen from this figure that the deformation pattern of the interface crack indicates that the thermal and mechanical loading cause the interface crack to shear and open. It can also be seen that the crack opening displacements increase with the increase in shear force. The amount of shear for Case 2 is smaller than the one for Case 1. The deformation pattern of load Step 6 in Case 2 is shown in Fig. 13. The overall deformation is larger with this load step than that shown in Fig. 10.

The variation of J-integral with shear force in this case is shown in Fig. 14. The value of J-integral is seen to increase with the increase in shear force. This is opposite to the trend in Case 1. Again the differences in values amongst the J-integrals calculated from the three paths are small, indicating that the J-integral is approximately independent of path. The three integration paths were the same as those used in Case 1.

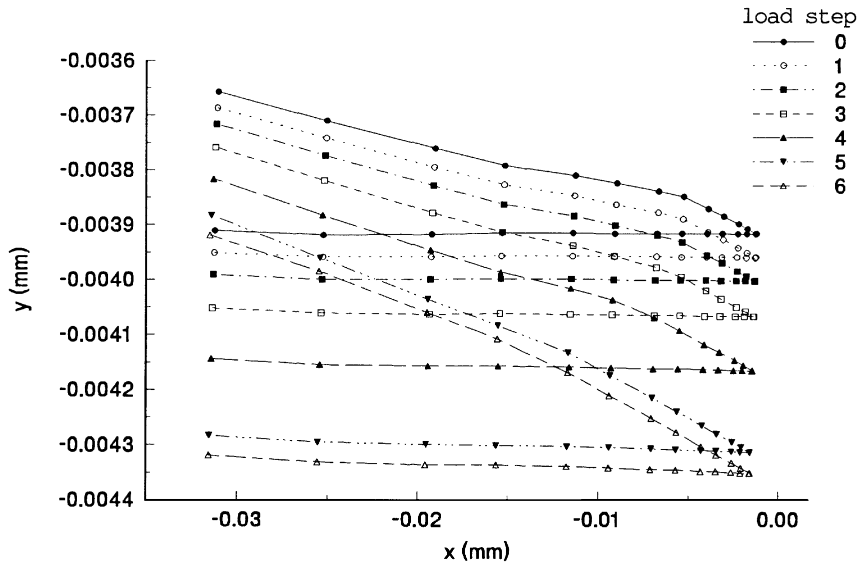

Fig. 12. Deformation of interface mesh for Case 2.

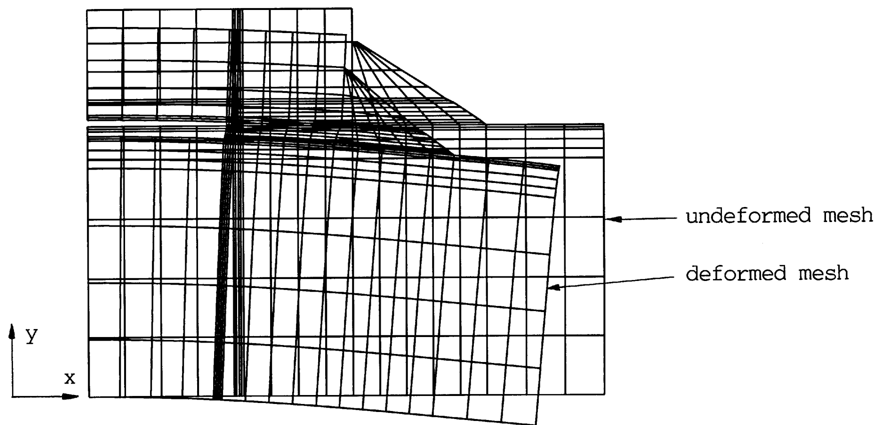

Fig. 13. Undeformed and deformed mesh for Case 2, load step 6.

Based on the J-integral theory described earlier, the value of the J-integral can reflect the stress and strain field ahead of a crack. It was explained earlier that the value of the J-integral decreases with increasing applied force for Case 1, i.e. the case with the crack at the resistor/solder interface. As for Case 2, i.e. the case with the crack at the solder/PCB interface, the value of J-integral decreases with increasing applied force. These results indicate that the case with the crack at the resistor/solder interface had decreasing stress and strain with the increase in shear force; whereas for the case with the crack at the solder/PCB interface, stress and strain increase with the increase in shear force. Consequently, a defect in the form of a crack at the solder/PCB interface is much more serious than a defect between the component and solder.

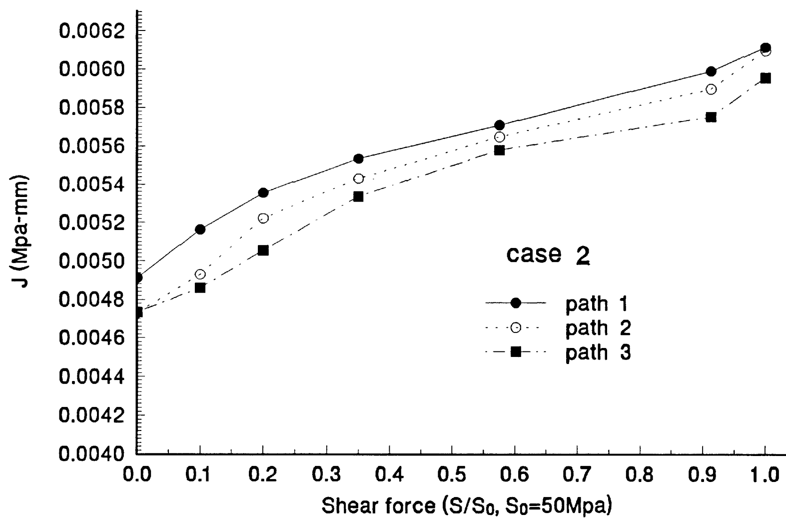

Fig. 14. Variation of J-Integral with shear force for Case 2.

5. Conclusion

The effect of cooling of a surface mount assembly containing interfacial cracks between solder and resistor and between solder and PCB was studied. The results indicated that the cooling caused the interface crack to shear and open. Large residual stress exists near the interface crack. From the value of the J-integral obtained, it can be estimated that a defect in the form of a crack at the solder/PCB interface is much more serious than a defect between the component and solder.

Acknowledgements

This research was supported by the University Grants Council of Hong Kong through research grant with number 9040161.

References

[1] T.R. Homa, Cracking of electronic packaging joints due to creep-fatigue, in: Proc. ASM's 3rd Conf. on Electronic Packaging and Corrosion in Microelectronics, 1987, pp. 209–216.

[2] W. Engelmaier, Effects of power cycling on leadless chip carrier mounting reliability and technology, Electronic Packaging and Production (1983) 58–63.

[3] J.T. Lynitt, M.R. Ford, A. Boetti, The effect of high dissipation components on the solder joints of ceramic chip carriers attached to thick film alumina substrates, IEEE Trans. Components, Hybrids, Manuf. Technol. 6 (1983) 237–245.

[4] J.M. Montante, D.R. Kling, High reliability attachment of multilayer chip carriers to ceramic substrates for the class S environment, in: Proc. Electronic Components Conf., 1984, pp. 129–137.

[5] D.L. Hallowell, D.W. Kellerman, Analysis of a stacked thick film package, in: Proc. Int. Microelectronics Symp. 1984, pp. 281–292.
[6] H. Danielsson, Chip carner on ceramic thick film multilayer boards in high reliability applications, in: Proc. Int. Microelectronics Symp. 1984, pp. 56–60.
[7] D.E. Riemer, C.W. Saulsberry, Power cycling of ceramic chip carriers on ceramic substrates (an analysis of test results), in: Proc. Int. Microelectronics Symp., 1984, pp. 480–485.
[8] G.V. Clatterbaugh, H.K. Charles, Jr., Thermomechanical behaviour of soldered interconnects for surface mounting: a comparison of theory and experiment, in: IEEE Proc. 34th Electronic Components Conf., 1985, pp. 60–72.
[9] J.H. Lau, D.W. Rice, P.A. Avery, Elastoplastic analysis of surface-mount solder joints, IEEE Trans. Components Hybrids, Manuf. Technol. 10 (1987) 346–357.
[10] S.E. Yamada, Elastic/plastic fracture analysis for bonded joints, Eng. Fracture Mech. 27 (1987) 315–328.
[11] S.E. Yamada, Time dependent crack growth in soldered joint, Eng. Fracture Mech. 28 (1987) 85–91.
[12] S.E. Yamada, A fracture mechanics approach to soldered joint cracking, in: IEEE Transs, Components Hybrids, Manuf. Technol. 12 (1989) 99–104.
[13] R.R. Klod Kokini, Reynolds, Transient heating vs cooling of interfacial cracks in ceramic-to-metal bonds, Eng. Fracture Mech. 38 (1991) 371–383.
[14] J.R. Rice, Elastic fracture concepts for interface cracks, J. Appl. Mech. Trans. ASME 55 (1988) 98–103.
[15] J.R. Rice, A path independent integral and the approximate analysis, J. Appl. Mech. Trans. ASME 35 (1968) 379–386.
[16] R.E. Smelser, M.E. Gurtin, On the J-integral for bimaterial bodies, Int. J. Fracture 13 (1977) 382–384.
[17] S.E. Yamada, The J-integral for augmented double cantilever beams and its application to bonded joints, Eng. Fracture Mech. 29 (1988) 673–682.
[18] J.A. King, Material Handbook for Hybrid Microelectronics, Artech House, Boston, 1988.
[19] D.J. Dean, Thermal Design of Electronic Circuit Boards and Packages, Electrochemical Publications, 1985.
[20] ABAQUS User's Manual, Hibbitt, Karlsson and Sorensen Inc., Providence, 1993.
[21] D.R.J. Owen, A.J. Fawkes, Engineering Fracture Mechanics: Numerical Methods and Applications, Pineridge Press, Swansea, UK, 1983.